

**Fermilab**

TM-1316  
SSC-N-12  
0102.000

A SIMULATION OF QUENCHES IN SSC MAGNETS  
WITH PASSIVE QUENCH PROTECTION

K. Koepke

June 1985

A SIMULATION OF QUENCHES IN SSC MAGNETS  
WITH PASSIVE QUENCH PROTECTION

K.Koepke

Introduction

The relative ease of protecting an SSC magnet following a quench and the implications of quench protection on magnet reliability and operation are necessary inputs in a rational magnet selection process. As it appears likely that the magnet selection will be made prior to full scale prototype testing, an alternative means is required to ascertain the surviveability of contending magnet types. This paper attempts to provide a basis for magnet selection by calculating the peak expected quench temperatures in the 3 T Design C magnet and the 6 T Design D magnet as a function of magnet length. A passive, "cold diode" protection system has been assumed. The relative merits of passive versus active protection systems have been discussed in a previous report (1). It is therefore assumed that - given the experience gained from the Tevatron system - that an active quench protection system can be employed to protect the magnets in the eventuality of unreliable cold diode function.

Quench Model

The calculations were performed with the program TMAX. As the magnet current decays during a quench, the program updates magnetic field, quench velocity, quench resistance and quench temperature for every magnet turn and uses the results to control the magnet current. Single or multiple quenches can be started anywhere in the magnet.

The quench velocities in the program are calculated with empirical equations obtained by fit to available velocity measurements. In the case of the Design C magnet, in situ velocity measurements - longitudinal and turn-to-turn - have been made (2) and are used unaltered in the program. In the Design D magnet case, the longitudinal velocities for the inner and outer cables have been measured in a test fixture (3). It can be shown - at least in the case of test magnet SBN003 - that longitudinal velocity measurements made in a magnet and in a test fixture agree on the 10 percent level (Table 1). Turn-to-turn quench delay data was obtained by scaling from data in test magnet SBN003 (4) and test magnet RO1001 (5).

The quench temperatures are obtained by equating the change in cable heat capacity to the heat deposition in the cable due to ohmic heating, i.e., from a Miit versus temperature calculation. This calculation ignores heat transfer (adiabatic approximation) across the boundary of the cable segment and must therefore be interpreted as the maximum cable temperature possible for a given ohmic heating. The validity of this approach has been tested by comparing an in situ measurement of cable temperatures (4) with the temperatures obtained from an adiabatic calculation (Fig.1). The comparison indicates that better agreement is obtained if the cable insulation is included with the heat capacity of the cable and this has been done in all subsequent calculations. The integration has neglected the contribution of the helium to the cable heat capacity. This assumption is probably correct for the Design C magnet which has solder filled cable. Its effect on the temperature calculation for the Design D magnet is also minimal. The program uses empirical quench velocities which already include the effect of the helium. In the case of the inner cable, the helium content of the cable increases the cable Miits necessary to reach a temperature of 700 K by approximately .1 Miit.

The number and location of quenches in a passively protected magnet have a strong relation to the peak quench temperature. Graded cable and magnetic field variations result in different quench velocities. Boundary conditions such as shims, coil boundaries and splices to stabilized conductors severely limit the extent of the normal quench zone. Multiple quenches in coils protected by more than one diode can give elevated temperatures due to the bias obtained from mutual coupling of the diode loops. In recognition of this fact, quench temperatures have been calculated for locations that result in the minimum and maximum temperature. It may be argued that the quench scenarios that result in maximum temperatures are unlikely or less likely to occur during normal operation. However, the loss of operation due to magnet replacement on an even infrequent basis is probably not tolerable.

The calculations have been made with the assumption that each magnet is part of a high series-impedance string which contains a constant current. This is equivalent to the requirement that the sum of the magnet current and the

bypass current is constant during the short interval that the current switches to the diode. This condition is approximately satisfied in the Design D circuit as the quench voltage rapidly overcomes the relatively low inductive voltage that results from the dump current decay. However, the dump time constant in the Design C circuit is small enough to result in significant current decay before the magnet resistance forces the bypass diodes to conduct. Nonetheless, the calculated temperatures are probably valid in the case of maximum current in the inner and outer coil. In this particular case, the initial current decay due to the dump circuit is roughly equal to the initial current decay in the quench simulation.

### Design C Magnet

The peak temperatures calculated for this magnet are shown in Fig. 2. Only the inner and outer coil temperatures were calculated as the trim coil operates at reduced current and its area and/or its composition can easily be changed if its quench temperatures are too high. Quenches were simulated in the body of the magnet where the quench is free to propagate in both longitudinal directions and also at the magnet end where the cable is spliced to the fully stabilized cable contiguous to the cold diode. The end-of-coil quench location for this magnet is critical because of the magnet's long turn-to-turn quench delay. This delay and the relatively small number of magnet turns available to the normal quench zone imply that most of the quench resistance comes from the first turn to quench. For quenches at the coil end, this quench resistance is halved. In the outer coil, the quench zone was limited to two turns. In the case of the inner coil, the third and fourth turn were simultaneously - and arbitrarily - quenched after 140 ms. The effects of intercoil quench propagation, or of multiple quenches in either or both coils were not investigated but are clearly relevant.

The cable and magnet parameters used in the quench simulation are courtesy of the TAC group. The cable cross section is shown in Fig. 3. Fig. 4 contains the calculated temperature versus Miits for this cable including the solder and insulation at 0 T and 3 T magnetic fields. The quench velocities, quench delays and coil inductances used are given in Table 2. The velocity and quench delay values for the 10.1 kA and 11.3 kA currents are extrapolated. The sizeable effect of iron saturation in this magnet has been approximated in the quench program by parameterizing the coil inductances as a function of ampere-turns.

## Design D Magnet

The peak temperatures calculated for this magnet are shown in Fig. 5 thru Fig. 7 as a function of magnet length and as a function of the number of protection diodes per magnet. In the case of single diode protection, the maximum quench temperature occurs for single quenches that start in the high field turn next to the coil key. At this quench location, the quench normal zone can only expand in one azimuthal direction which compensates for the higher quench velocities. For magnets with multiple diode protection as shown in the figures, the maximum quench temperature occurs for dual quenches at the median plane of the magnet. In general, geometrically symmetric and simultaneous quenches with mutually coupled decay circuits behave as if the coil inductance per quench is  $L/2$  instead of  $L/(2+2*k)$  where  $L$  and  $k$  are the total magnet inductance and mutual coupling constant respectively. End-of-coil quenches for this magnet were not considered because of the relatively fast turn-to-turn quench propagation and the large number of magnet turns that contribute to the quench normal zone. This assumes that the magnet ends are of minimum size which allows a quench to rapidly exit from this location. If exaggerated "dog bone" ends are used, the magnet end quench protection will need to be reevaluated.

The quench calculations assumed that the Design D magnet utilizes the cables specified for the Design A magnet of the SSC design study (6) and that the coil geometry agrees with BNL drawing no. 22-00217-4 Rev B. Fig. 8 gives the calculated temperature versus Miits for these conductors at field values of 0 T and 6 T. The Miit integration includes a .004 in. thickness of Kapton insulation per cable. The inner and outer longitudinal quench velocities used are plotted in Fig. 9 and Fig. 10. These velocities were measured in a test fixture and were furnished by B. Sampson, BNL. The turn-to-turn quench delays were obtained by scaling from measurements in test magnet SBN003 (A. Prodell, et al., BNL) and test magnet R01001 (K. Koepke, et al., FNAL) and are shown in Fig. 11. The magnet inductances were taken from SSC publication SSC-MD-104 (J. Cottingham) without any adjustment for the small iron saturation.

## Adjustments

The quench temperatures calculated should be considered as a first approximation calculation as many factors present in a quenching magnet have been ignored. For example, the quench velocities were measured at constant current and field. It is known that during a quench, these velocities are increased due to eddy current heating. In fact, Tevatron dipoles quench spontaneously near short sample at 300 A/s. Other effects which may significantly alter the quench temperatures are eddy currents in the collars and cryostat - especially if constructed out of aluminum - and quench propagation between inner and outer coils. If included, these effects would tend to lower the actual quench temperature calculated. These effects, along with the asymptotic behavior of the quench velocity near short sample, are probably also responsible for the maximum in quench Miits observed in passively protected magnets, e.g., the CBA magnets. This maximum in quench Miits occurs at magnet currents well below the short sample current for the cable in the magnet.

A more realistic peak temperature estimate can be obtained by assuming a higher initial "effective quench velocity", or by evaluating the quench temperature at the magnet current at which the Miit maximum is observed, or by adjusting the calculated quench Miits by an observed correction factor. We can obtain an estimate of the current at which the quench Miits of the inner Design D coil will be at a maximum by scaling the current at which the quench Miits for the inner coil of test magnet SBN003 peaked. Scaling by cable cross section areas yields a current of 4450 A. When the inner coil Design D quench temperatures are evaluated at 4450 A, the result is equal to 78 % of the result obtained at 5906 A. This correction is probably not universal, i.e., it may depend on magnet length and certainly is different for different magnets.

## Conclusions

Superconducting cable formed out of niobium-titanium with Kapton film insulation starts to show short sample degradation at a quench temperature of 800 K. Repetitive quenches in solder-filled cable may show damage at even lower temperatures. If we arbitrary set the allowed quench temperature to 700 K, this quench temperature limit and the calculated quench temperatures can be used to evaluate the relative suitability of passive quench protection for the magnets discussed.

Arbitrarily using the same correction factor for the inner and outer coils of both magnets, it appears that the 140 m long 3 T magnet and the 16.6 m long 6 T magnet are protectable with a passive quench protection system. The 3 T magnet requires a minimum of 6 diodes per half cell. This assumes that a pair of parallel diodes are needed to carry the order 10 kA currents in the inner and outer bus. A single diode for the trim winding and another for the separate quadrupole are also assumed. The 6 T magnet requires 21 diodes per 100 m half cell, i.e., 4 diodes per 16.6 m dipole and one diode for the separate quadrupole. As the 3 T ring needs to be twice as long, the 6 T ring needs approximately 2.8 times as many diodes per aperture for passive quench protection. A more complete comparison among competing SSC magnets from the viewpoint of quench detection and protection has been made in a previous report (1).

#### References

1. WORKSHOP ON SSC COMMISSIONING AND OPERATIONS, Systems Group, "Quench Detection And Protection", K. Koepke and G. Tool
2. private communication, J. Ziegler, TAC
3. private communication, W.B. Sampson, BNL
4. private communication, A. Prodell, BNL
5. unpublished, K. Koepke, FNAL
6. SUPERCONDUCTING SUPER COLLIDER, Reference Design Study for U.S. Dept. of Energy, May 8, 1984

Table 1

A comparison of the longitudinal velocities measured in a test fixture (W.B.Sampson, BNL) to the longitudinal velocities measured in test magnet SBN003 (A. Prodell, BNL). The cable in both instances was 1.3/1 high homogeneity NbTi with a cross section of .085 sqcm.

Coil Current (amps)	Average Field (tesla)	SBN003 Velocity (m/sec)	Fixture Velocity (m/sec)
Quench origin - inner coil, median plane (IMPL)			
1500	1.69	1.6	1.34
2500	2.82	2.7	3.15
3000	3.38	4.6	4.56
3500	3.94	6.3	6.02
4000	4.5	8.4	8.09
Quench origin - inner coil, median plane end (IEL)			
1500	1.69	1.5	1.34
2500	2.82	2.8	3.15
3000	3.38	5.0	4.56
4000	4.5	11.0	8.09
Quench origin - outer coil, median plane end (OEL)			
2000	.65	1.7	1.6
3000	.97	3.2	3.16
4000	1.3	5.0	5.6
5000	1.62	7.7	8.9
5500	1.79	10.0	10.5
Quench origin - outer coil, median plane (OMPL)			
2000	.65	3.6	1.6
3000	.97	6.7	3.16
4000	1.3	10.4	5.6
5000	1.62	15.4	8.9
5500	1.79	18.8	10.5

Last data set has insidious factor of 2 ?

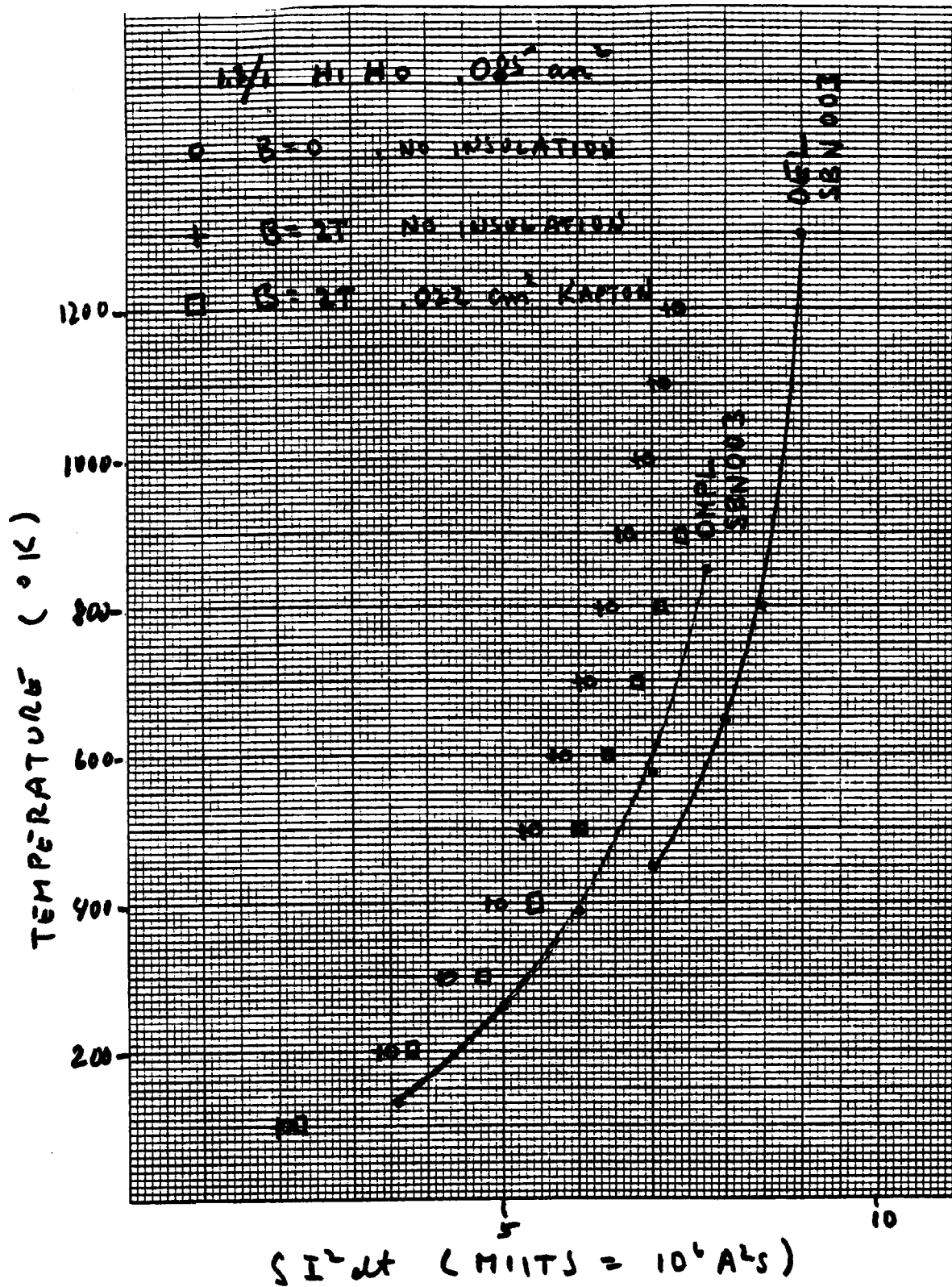


Fig.1 Calculated Temperature versus Miits values compared to the measured temperatures in magnet SBN003. The OMPL location is in the outer coil on the median plane approximately 34 in. from the end of the coil. The OEL location is the same turn but in the "dog bone" end.

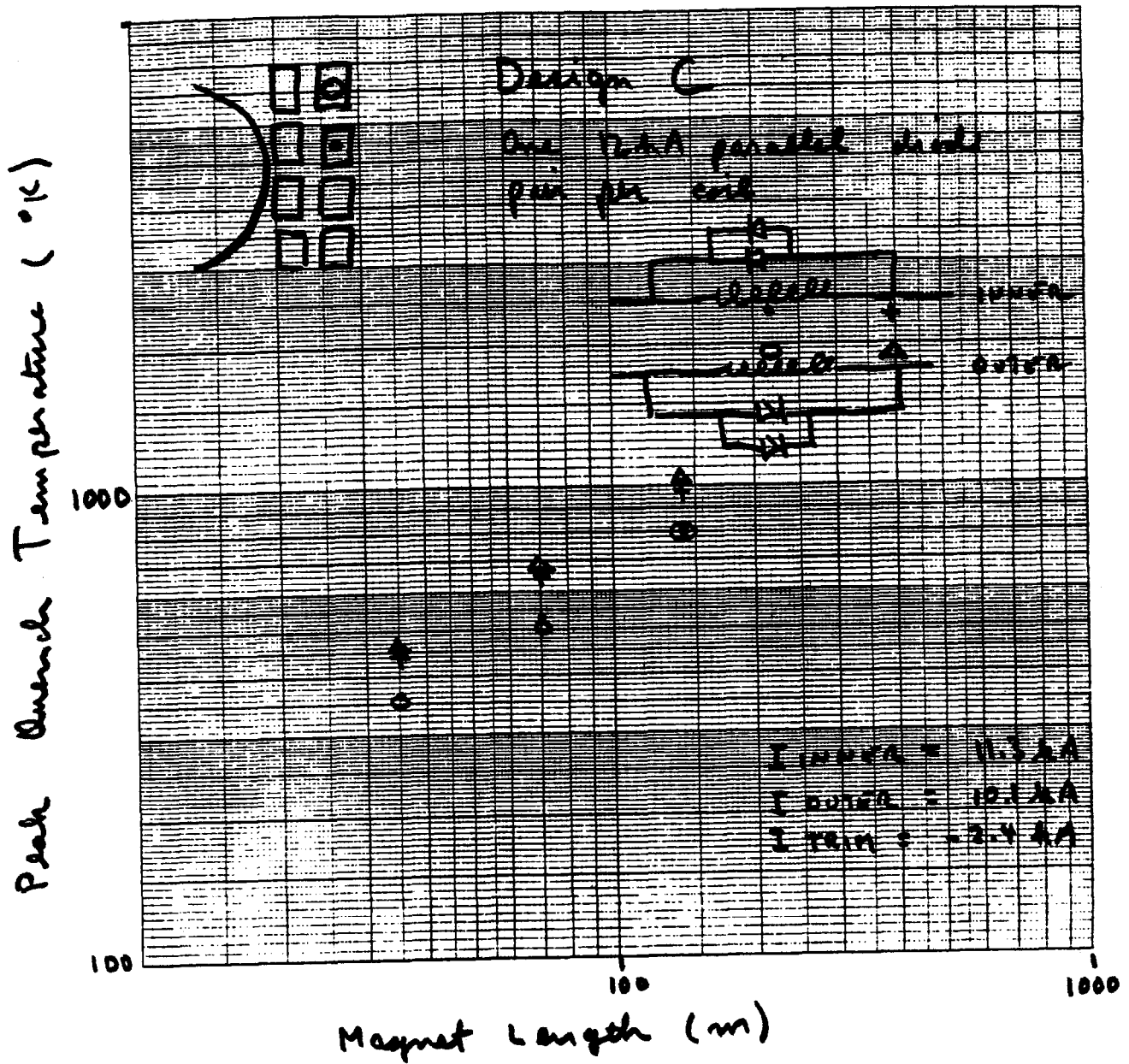
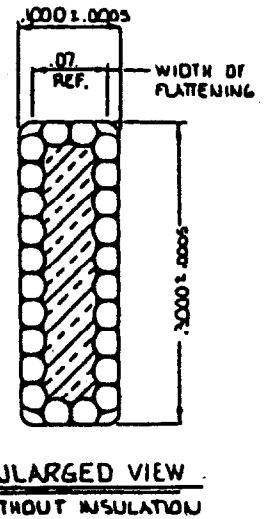
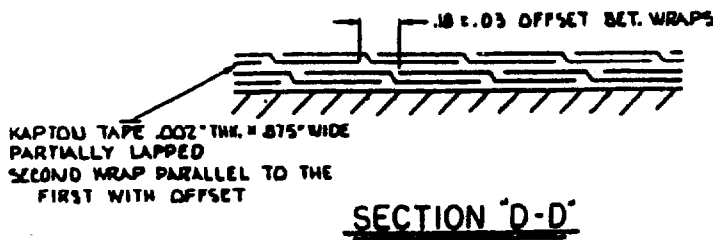
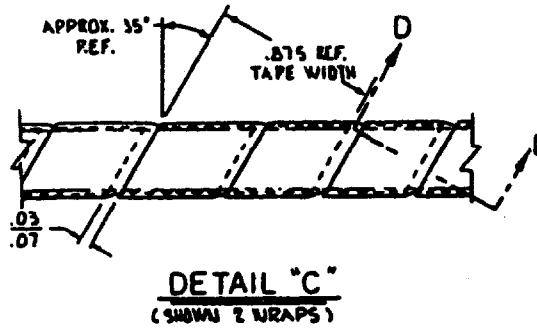
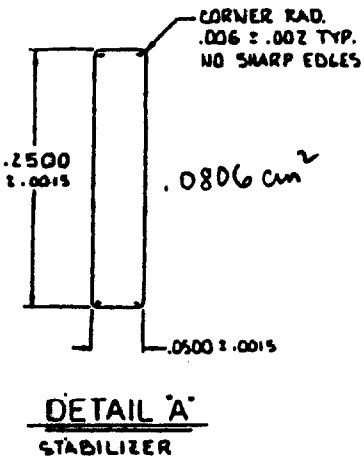
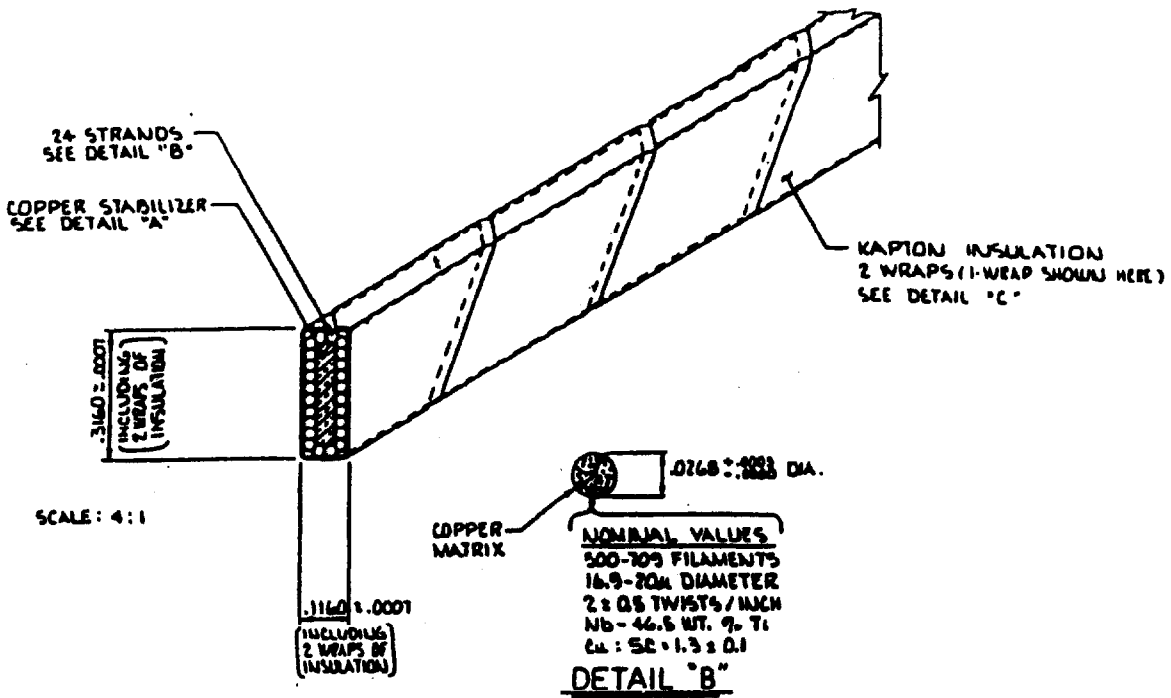


Fig.2 Calculated maximum quench temperatures for the 3 T TAC magnet. The actual quench temperatures can be expected to be lower (See "Adjustments" of text).



NOTES:

1. CABLE PITCH - 3.6 INCH. NOMINAL - MAY BE VARIED TO ACHIEVE SINGL LAY OF THE STRANDS.
2. CABLE SOLDER FILLED. SOLDER : TIN - 5% SILVER
3. CABLE ROLLED BY TURK'S HEAD BEFORE AND AFTER SOLDERING.
4. OPERATING CONDITIONS : I = 12 KA, B = 5.5T, T = 4.5K

Fig.3 Cable parameters for the 3 T magnet as used in the quench calculations.

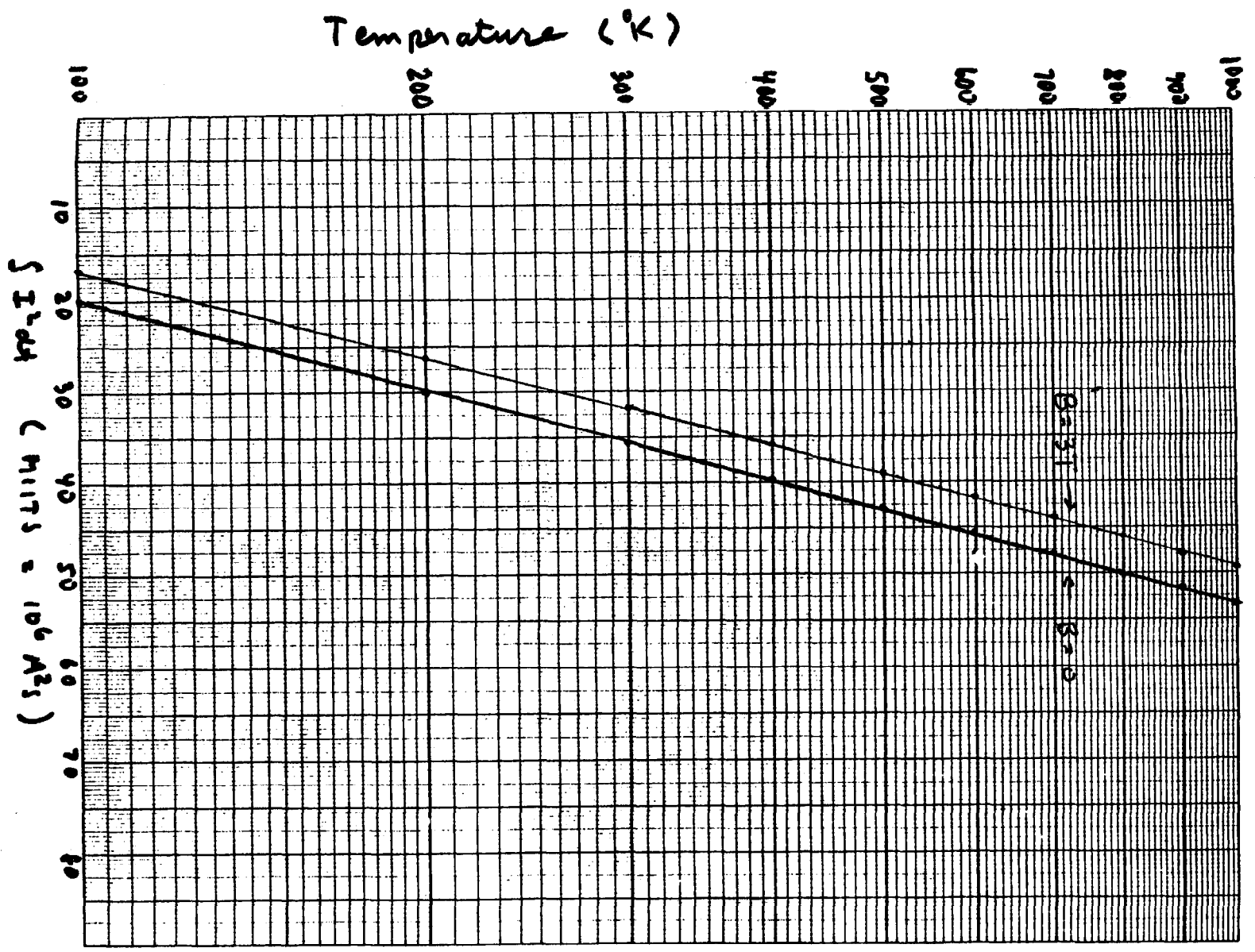


Fig.4 Predicted peak quench temperature versus Mitrs for the 3 T magnet cable as calculated by TMAX.

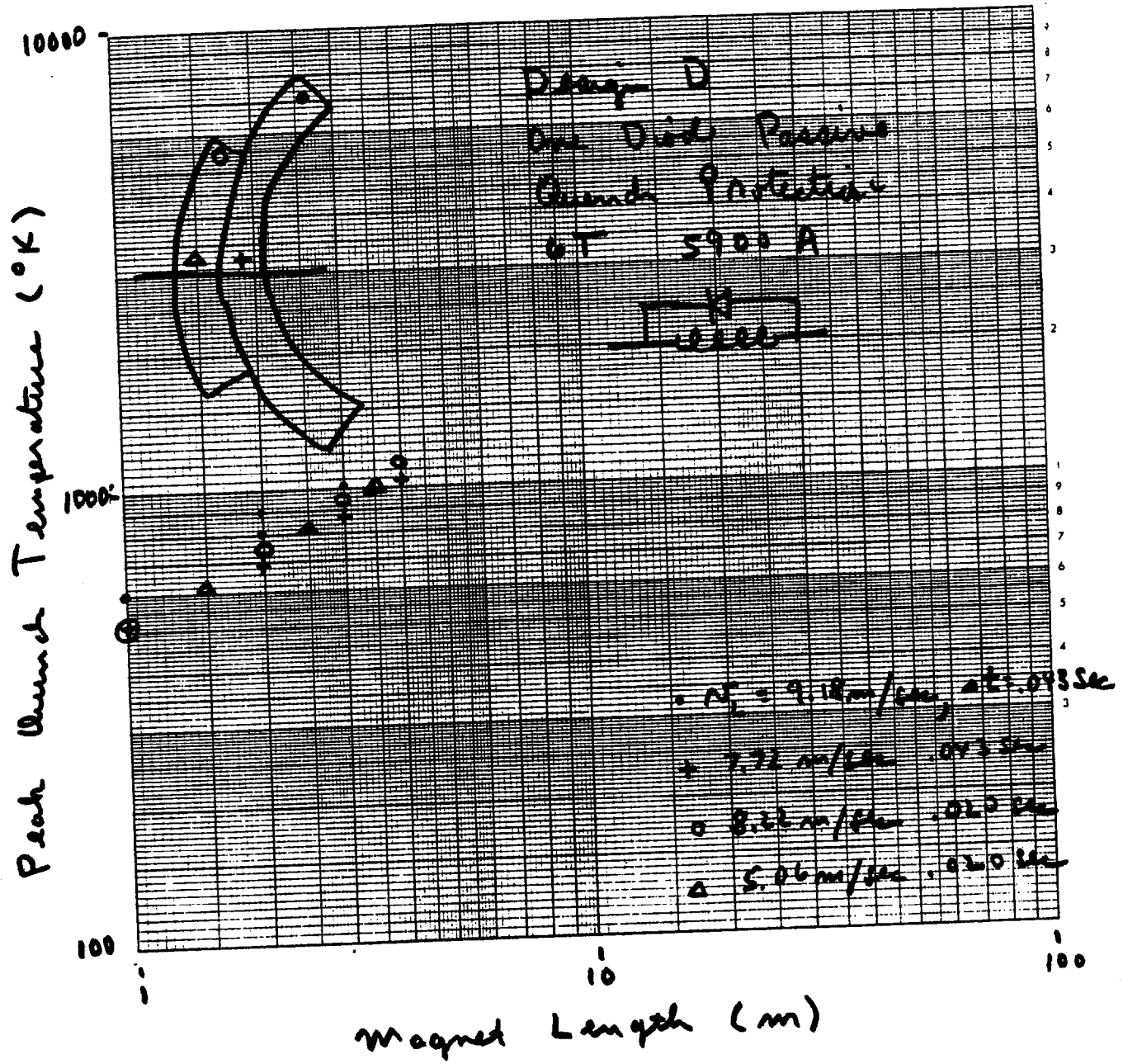


Fig.5 Calculated maximum quench temperatures for the 6 T magnet with single diode protection. The actual quench temperatures can be expected to be lower (See "Adjustments" of text).

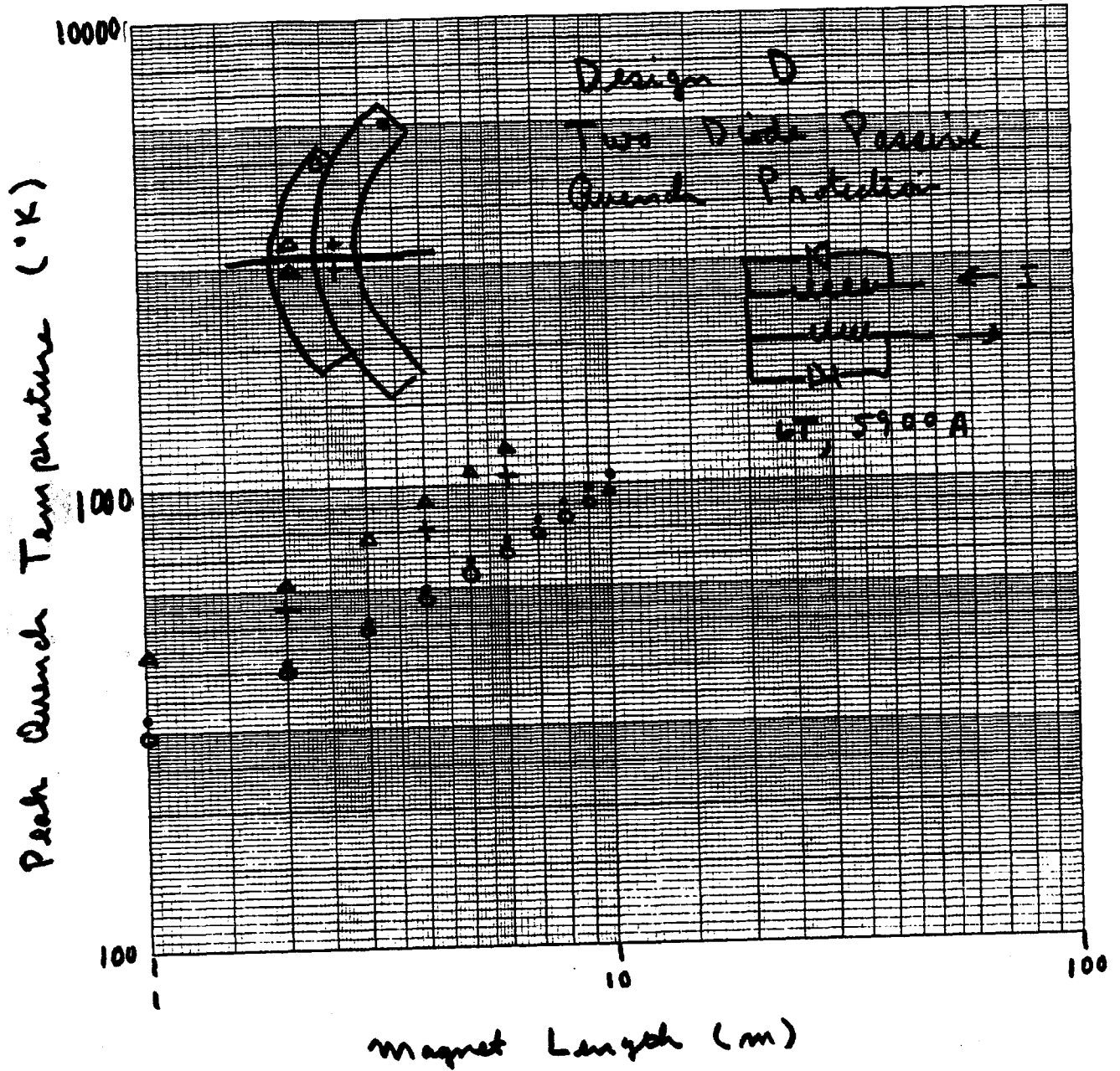


Fig.6 Calculated maximum quench temperatures for the 6 T magnet with two diode protection. The actual quench temperatures can be expected to be lower (See "Adjustments" of text).

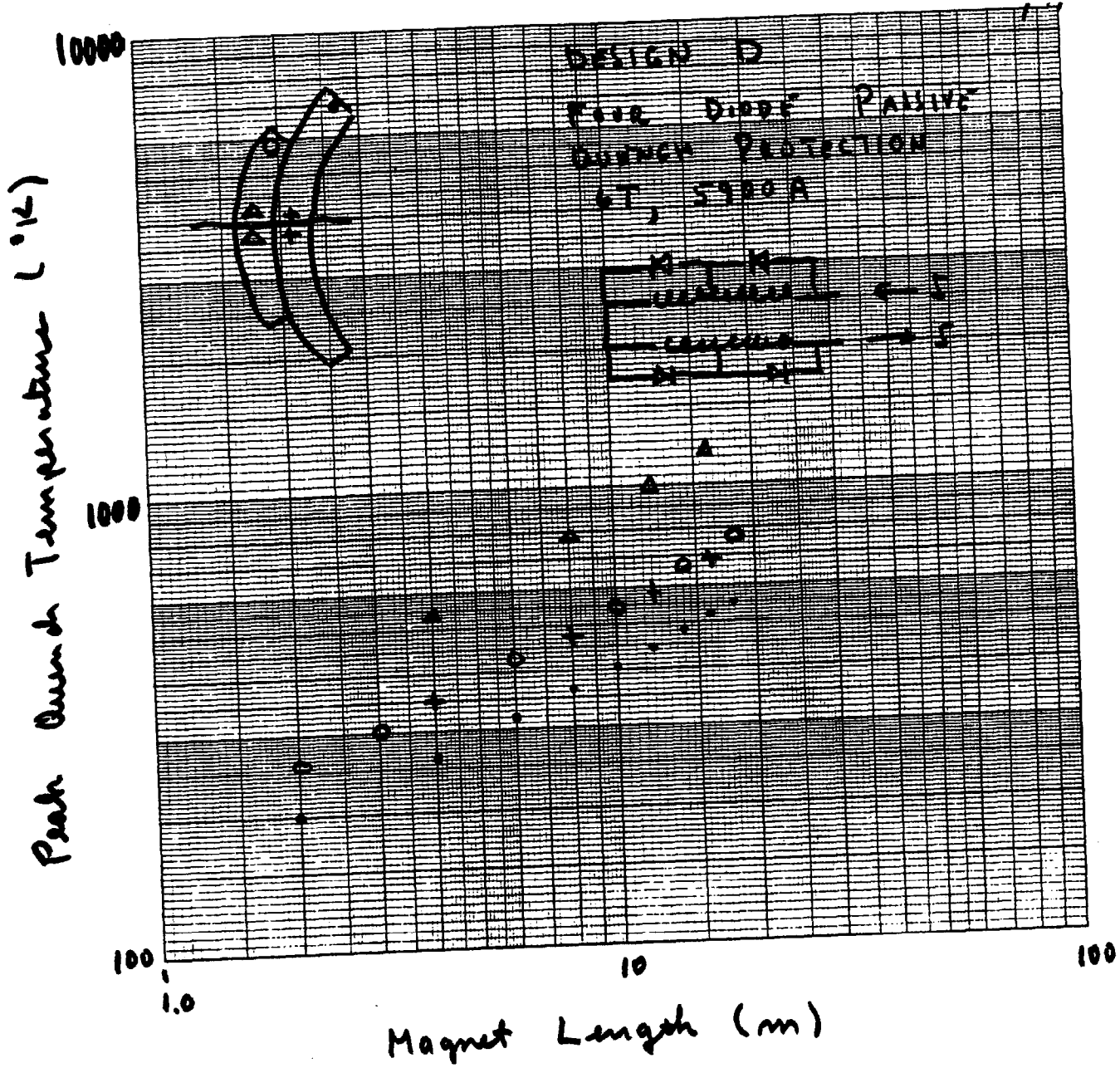


Fig.7 Calculated maximum quench temperatures for the 6 T magnet with four diode protection. The actual quench temperatures can be expected to be lower (See "Adjustments" of text).

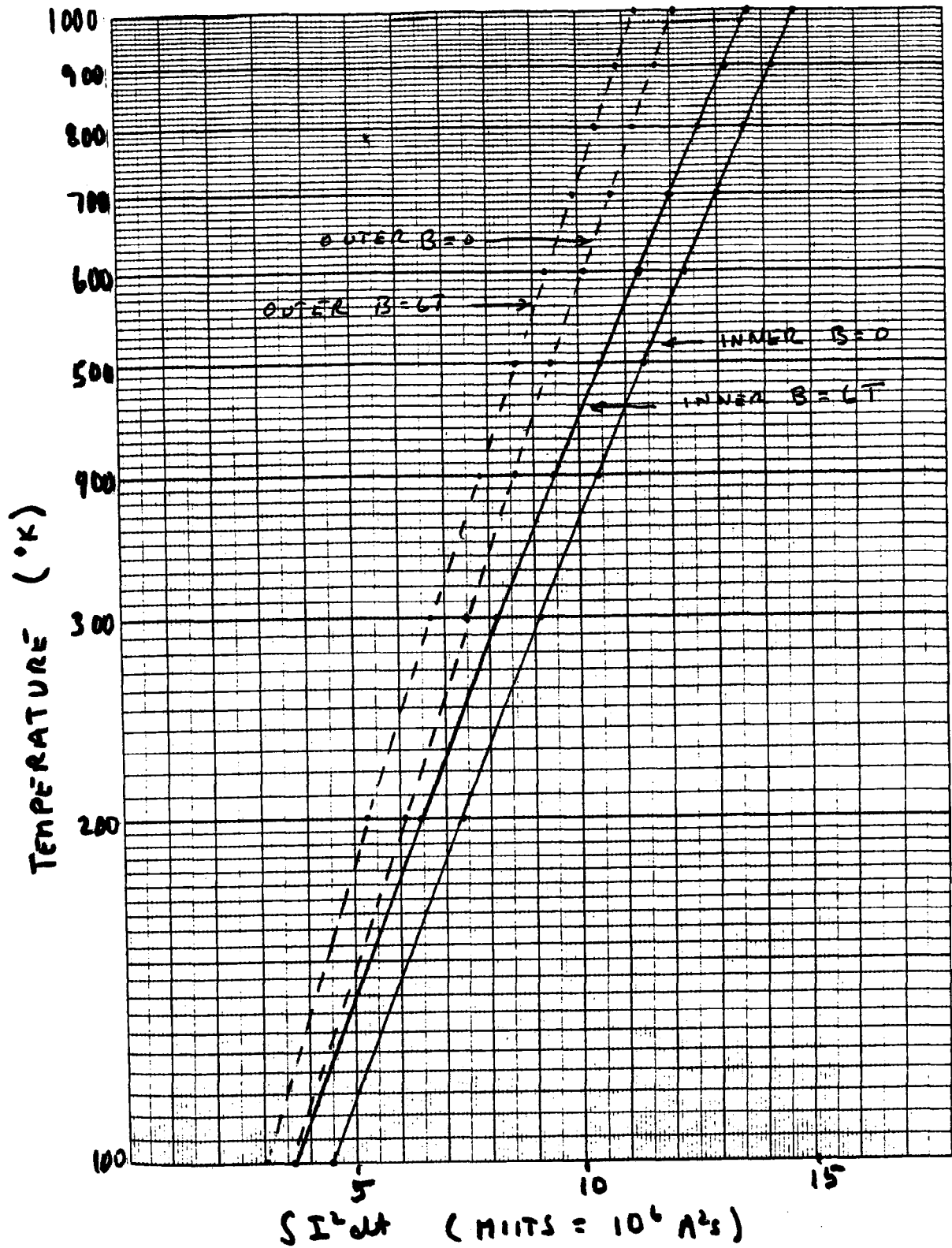


Fig.8 Predicted peak quench temperature versus Miits for the 6 T magnet cable as calculated by TMAX.

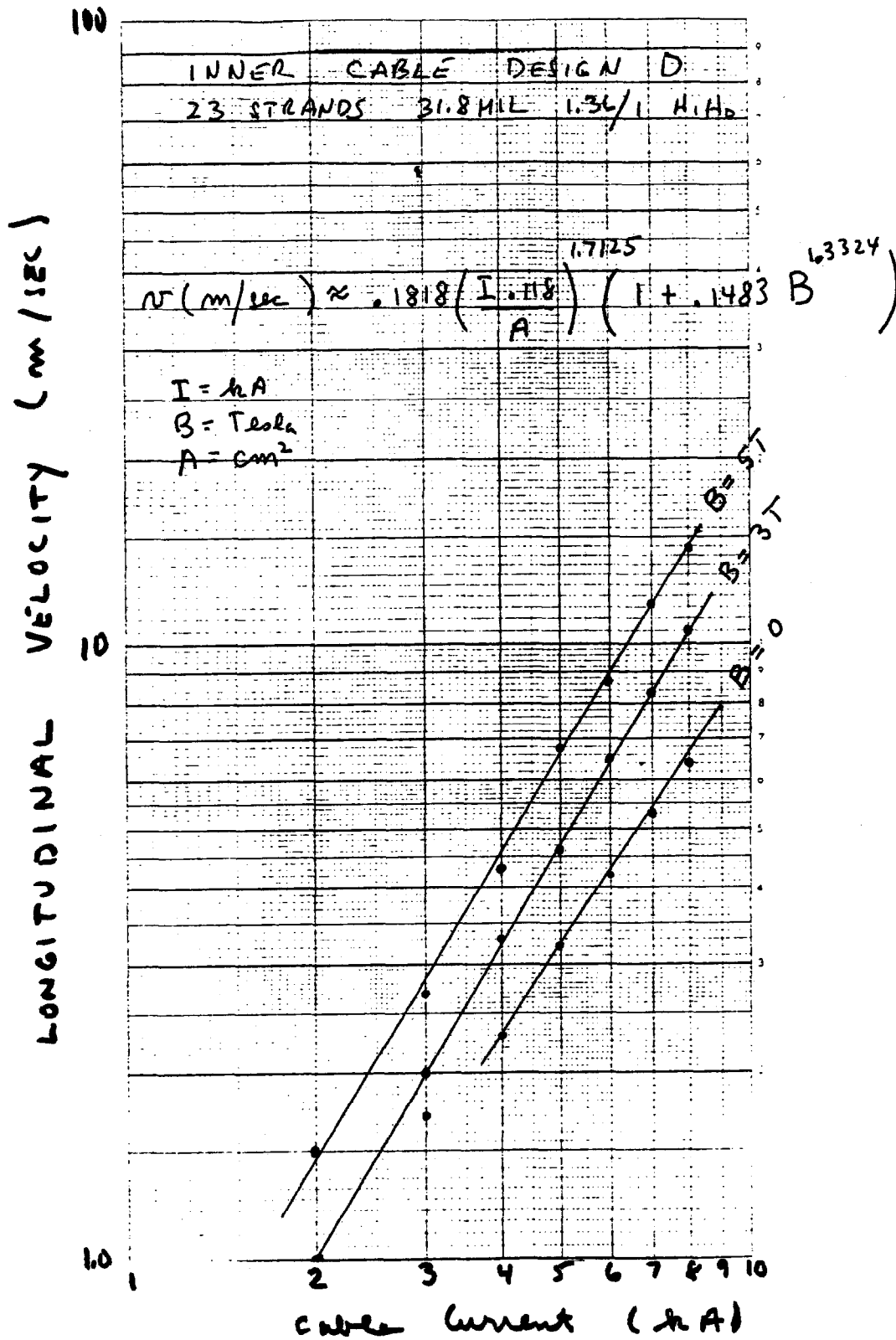


Fig. 9 Quench velocities used for the inner coil of the 6 T magnet (Ref. 3).

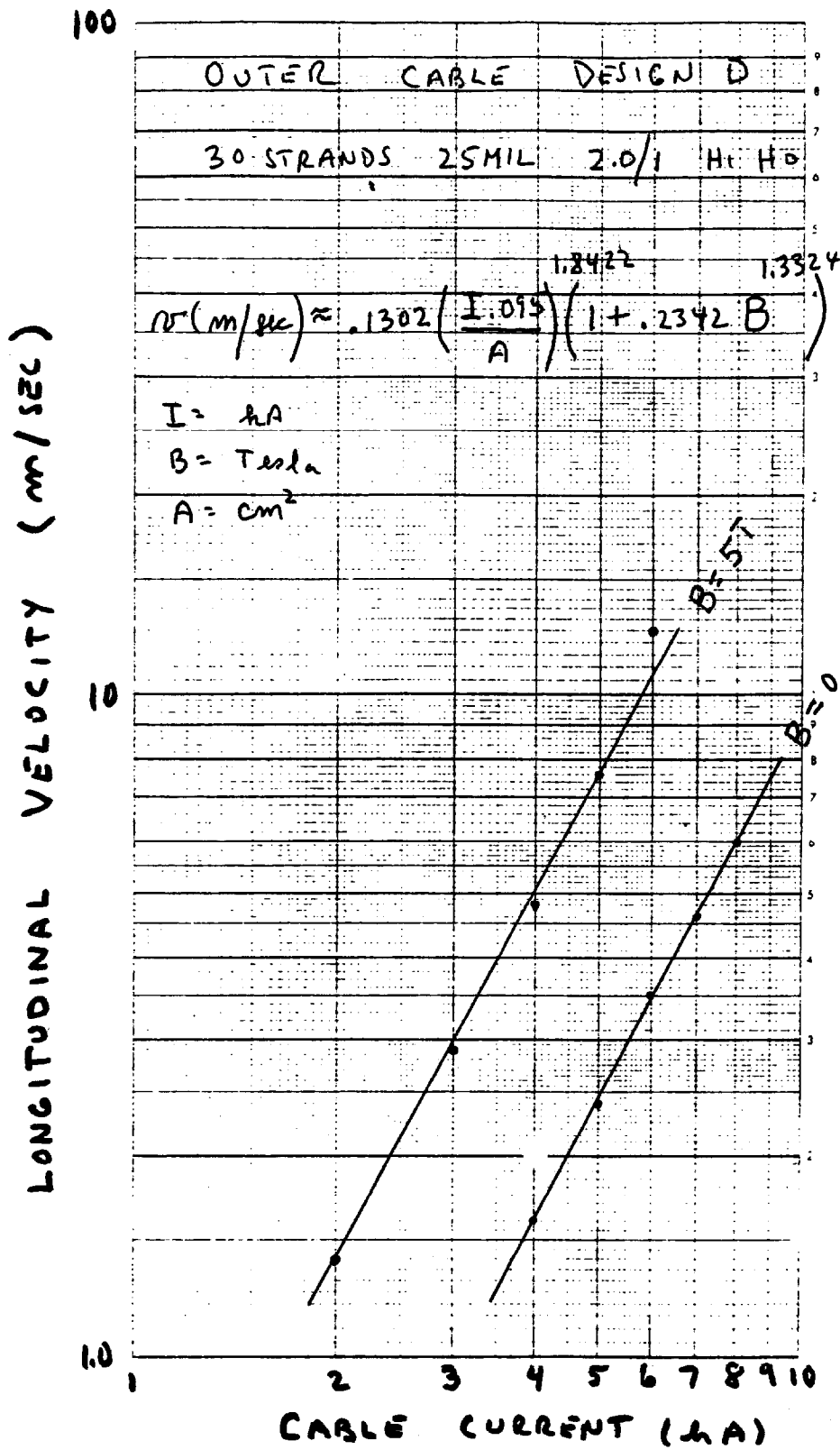


Fig.10 Quench velocities used for the outer coil of the 6 T magnet (Ref. 3).

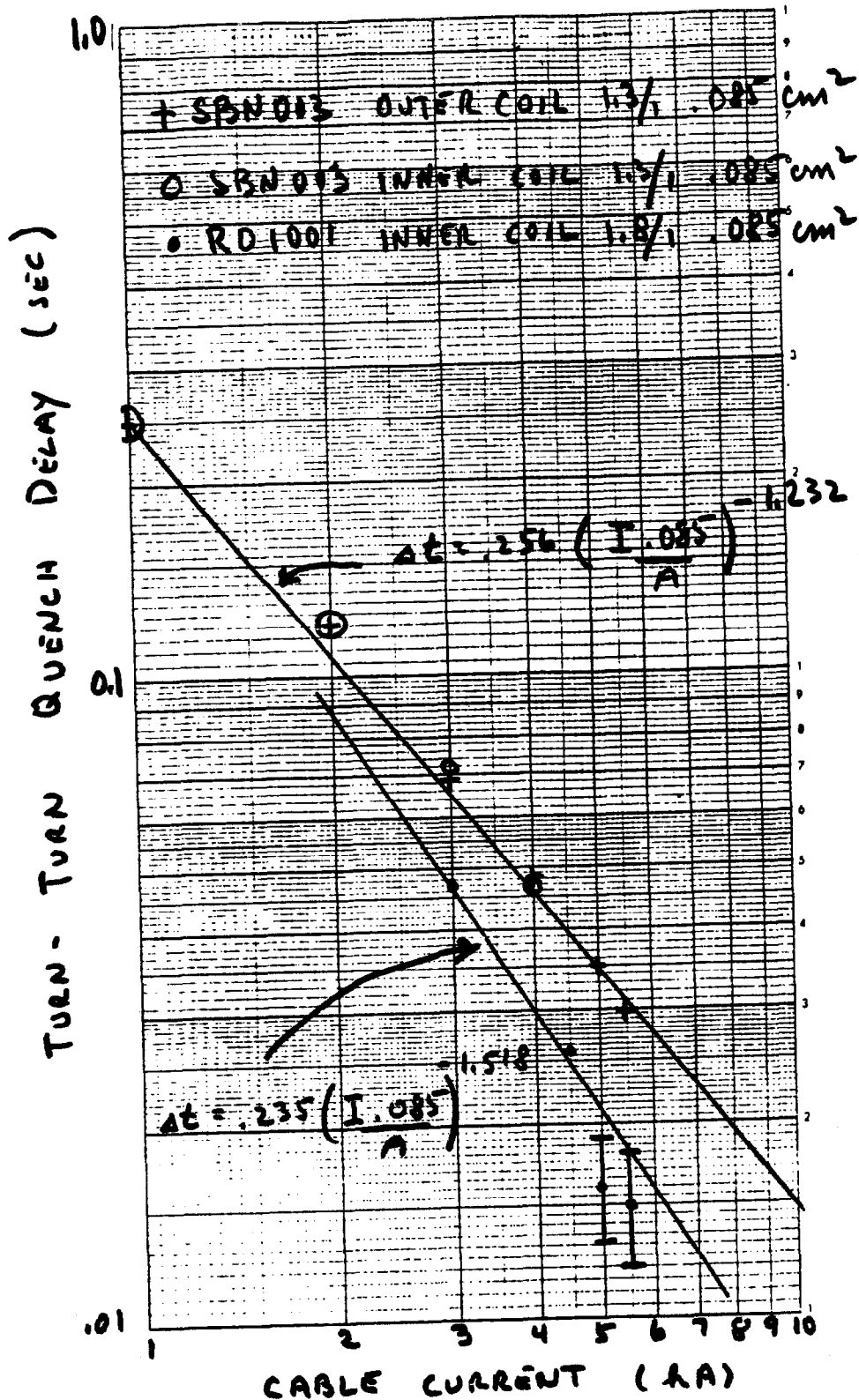


Fig. 11 Turn to turn quench delays used for the inner and outer coil of the 6 T magnet (Ref. 4,5)